Adsorption and photocatalytic decolorization of a synthetic dye erythrosine on anatase TiO$_2$ and ZnO surfaces

M.A. Hasnat [a,*], M.M. Uddin [a], A.J.F. Samed [a], S.S. Alam [a], S. Hossain [b]

[a] *Department of Chemistry, Shahjalal University of Science and Technology, Sylhet-3114, Bangladesh*
[b] *Bangladesh Atomic Energy commission, Savar, Dhaka, Bangladesh*

Abstract

The UV radiation assisted photocatalytic decolorization/degradation kinetics of an anionic dye erythrosine (ER), has been studied over TiO$_2$ and ZnO surfaces. Since adsorption is the prerequisite condition for decolorization/degradation of dye molecules in presence of heterogeneous catalysis, the Langmuir and Freundlich isotherms were examined to verify the adsorption intensity. Standard adsorption free energy measurement implies that the adsorption of ER on both TiO$_2$ and ZnO surfaces is spontaneous endothermic process. The effect of catalyst loading (TiO$_2$/ZnO) revealed the fact that the maximum decolorization rate is obtained under an optimized catalyst loading condition. The decolorization efficiency was also investigated over the pH range of 5.0–10.0 indicating that increasing pH enhances decolorization efficiency. The influence of H$_2$O$_2$ on decolorization efficiency was found noticeable since it is a hydroxyl radical provider. The kinetic study of this degradation indicates that under the experimental condition, the decolorization mechanism follows zero order kinetics on the basis of Langmuir–Hinshelwood (L–H) heterogeneous reaction mechanism.
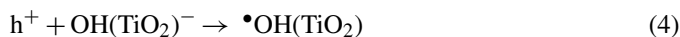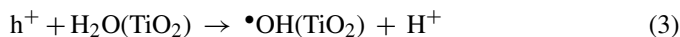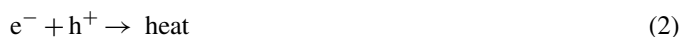
1. Introduction

Numerous biodegradability studies on dyes have shown that azo dyes are not likely to be biodegradable under aerobic condition [1–3]. Extensive researches are being carried out world wide to degraded organic pollutants using semiconductor type photocatalysts namely TiO$_2$, ZnO and so on [4–9]. Recently, we reported adsorption and degradation of a cationic dye and an anionic dye using TiO$_2$ catalyst [10,11]. Heterogeneous photo catalysis is an effective method for organic pollutants containing wastewater treatment as it completely mineralizes the organic pollutants [9,10]. Among the semiconductor photocatalysts available, TiO$_2$ and ZnO are extensively used due to their properties like resistance to photo corrosion, less expensive, nontoxic and the use of them at ambient conditions [5–12]. Alok Mittal etl used organic type adsorbents bottom ash and de-oiled Soya as adsorbents in removal of erythrosine from aqueous medium [13]. Yu Yang and co-workers reported photocatalytic degradation mechanism of several dye components including erythrosine using macro porous hybrid taitania [14]. In this study, we have demonstrated the relative adsorption and decolorization kinetics of a textile dye erythrosine (ER) which is generously applied in different dying industries using heterogeneous photo-catalysts TiO$_2$ and ZnO.

Fig. 1 indicates molecular structure of ER. The decolorization/degradation reaction is a complex mechanism. Decolorization of dye molecules occur either by some reversible/irreversible structural changes or by complete degradation of the dye molecules [4–10].

TiO$_2$ catalyzed decolorization/degradation mechanism of dye (D) molecules in presence of UV radiation is described by the mechanism given bellow [15]:

$$TiO_2 + h\nu \rightarrow e^- + h^+ \tag{1}$$

$$e^- + h^+ \rightarrow heat \tag{2}$$

$$h^+ + H_2O(TiO_2) \rightarrow {}^\bullet OH(TiO_2) + H^+ \tag{3}$$

$$h^+ + OH(TiO_2)^- \rightarrow {}^\bullet OH(TiO_2) \tag{4}$$

* Corresponding author. Tel.: +81 96 343 7160.
  E-mail addresses: mahtazim@yahoo.com, mah-che@sust.edu
(M.A. Hasnat).
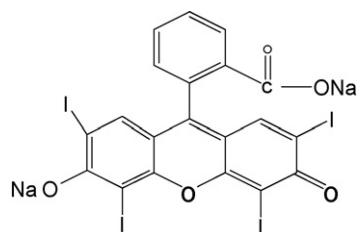
Fig. 1. Molecular structure of erythrosine.

$$e^- + O_2 \rightarrow O_2^{\bullet-} \tag{5}$$

$$O_2^{\bullet-} + HO_2^{\bullet} + H^+ \rightarrow H_2O_2 + O_2 \tag{6}$$

$$^{\bullet}OH(TiO_2) + D \rightarrow \text{intermediates} \rightarrow P \tag{7}$$
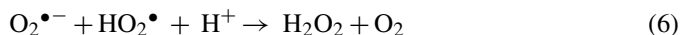
The mechanism suggests that the dye molecules are first adsorbed on TiO$_2$ surface then under illumination by UV radiation, one electron is promoted from conduction band to the valence band of the TiO$_2$ generating e$^-$/h$^+$ pair. The action of the e$^-$/h$^+$ pair is terminated by degrading dye molecules (D) into products (P) through intermediate formation and generating heating effect through a complex reaction. ZnO dispersion has almost the similar photocatalytic activity in presence of UV radiation [16].

2. Experimental

2.1. Materials

Erythrosine (ER^{2-}) is an anionic textile dye (molecular formula C$_{20}$H$_6$O$_5$I$_4$Na$_2$) was supplied by Aldrich. Anatase TiO$_2$ ((Degussa, P25 having specific surface area of 50 m^2/g and band gap energy of 3.2 eV) and ZnO (Fluka, having surface area of 100 m^2/g with band gap energy of 3.37 eV) were applied as semiconductor photocatalysts. Supporting NaOH and HCl (Merck) were also used to maintain pH.

2.2. Apparatus

All the experiments were done in open air and at room temperature (299 K). Fig. 2 shows the experimental setup in order to carry out the photolysis of catalyst containing reaction mixture. The reaction mixture was kept in a reactor (a cylindrical Pyrex vessel of 5 cm. diameter with capacity of 50 mL) positioned at 10 cm apart from the light source. In order to maintain the room temperature, the vessel was surrounded by a water jacket, consisting of one inlet and another outlet for the passage of cold water. The reactor contained a stirring rod supported by a magnetic stirrer to confirm homogeneity of the reaction mixture throughout the reactor. The light source used was a low-pressure mercury lamp (PASCO scientific, Hg light source OS-9286) of 125 W and web length of 200–400 nm. The change in concentration of the dye molecules in solution was measured spectrophotometrically using a Shimadzu-160 double beam spectrophotometer. pH of the solutions were adjusted by an Orion pH meter.
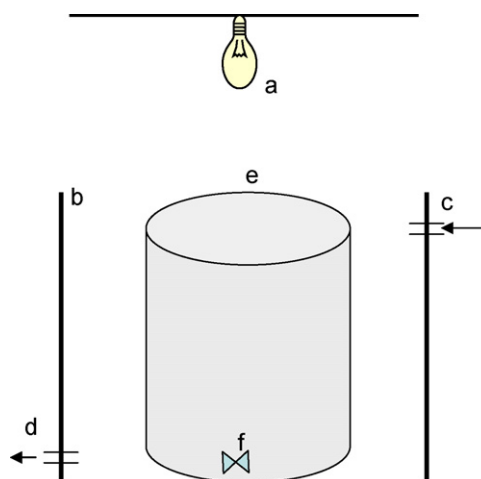

Fig. 2. Experimental setup of the reactor. (a) Light source, (b) water jacket, (c) water inlet, (d) water outlet, (e) cylindrical Pyrex vessel (2r: 4 cm; h: 5 cm) and (f) magnetic stirrer.

2.3. Experimental procedure

In order to evaluate the effect of different effectual parameters, batch experiments were carried out. For every single experiment, the aqueous suspension was prepared by adding a requisite amount of ZnO/TiO$_2$ in a 50 mL volumetric flask containing little water and then erythrosine (ER) solution was added to the volumetric flask in such a way that the final concentration of the solution becomes the desired one. pH was adjusted by adding 0.01 M HCl or 0.01 M NaOH. Then the solution was stirred by a magnetic stirrer for 30 min. After that the reaction mixture was kept overnight in a dark chamber to reach adsorption desorption equilibrium. The reaction mixture was then photolyzed for a fixed time. During photolysis, 2.0 mL sample from the reactor was withdrawn at regular intervals for analysis. The withdrawal sample was first centrifuged at 3500 rpm for 12 min and then filtered with a filter paper (grade: 474) to remove catalyst particles completely. The transparent solution was then inserted into the spectrometer for spectral studies and concentration measurement. ER has absorption peaks at 261, 306 and 526 nm. The peaks at 261 and 306 nm are due to aromatic parts of ER and peak at 526 nm (molar absorption coefficient, $\epsilon_{max} = 7.24 \times 10^4$ L mol^{-1} cm^{-1}) is due to color of the ER molecules. We have measured decolorization at 526 nm only though we have noticed the removal of aromatic peaks due to degradation (spectral changes not shown).

3. Result and discussion

3.1. Study of adsorption isotherms and thermodynamics

Adsorption is the major prerequisite condition for any heterogeneous catalysis reaction.

Zero point charge (ZPC) value of TiO$_2$ and ZnO semiconductors are at pH of ca. 6.5 and 10.0, respectively. Therefore, surfaces of both of the semiconductors are positively in the acidic pH and negatively charged above respective ZPC pH.

Since ER is an anionic dye, therefore, ER should show the most effective adsorption in the acidic pH. ER shows its structural stability in the pH range of 4.8–11.5. We observed that pH range 5.0–6.8 showed the best relative adsorption behaviors by the both catalysts. In order to study adsorption behavior, the Langmuir isotherm and Freundlich isotherm models were verified at a pH ca. 6.0.

The Langmuir adsorption isotherm, in case of ER adsorption on TiO$_2$/ZnO surface, can be expressed by Eq. (8):

$$\frac{[ER]}{q_e} = \frac{[ER]}{K'} + \frac{1}{K'k_1} \tag{8}$$

where, [ER] is the equilibrium concentration of erythrosine (mg/L), q_e (mg/g) the amount of ER adsorbed by per unit mass of ZnO or TiO$_2$, K' and k_1 are the Langmuir constants related to adsorption capacity and energy of adsorption, respectively. Freundlich isotherm (Fig. 3) explains the relation between qe and equilibrium ER concentration (Eq. (9)):

$$\ln q_e = \ln K_F + 1/n \ln[ER] \tag{9}$$

The Freundlich adsorption isotherm usually is applied to the highly heterogeneous surfaces [14–16]. The empirical constant K_F refers to the relative adsorption capacity and 'n' represents adsorption intensity under different experimental conditions. Based on Eqs. (8) and (9), the values of the empirical constants (Table 1) for both isotherms indicate that our experimental data agrees well with the Langmuir and Freundlich models at 299 K. In Fig. 3, the lacking of plateau may be due to the formation of potential multilayer.

The adsorption property can also be explained by calculating thermodynamic parameters. In order to calculate thermodynamic parameter, the standard adsorption free energy ($\Delta_{ad}G°$), experiments were carried out using variable initial ER concentrations (8.0–26.0 μM). Under constant temperature condition, equilibrium adsorption constant (K_0) is defined by the Eq. (10):

$$k_0 = \frac{a_s}{a_e} = \frac{f_s}{f_e}\frac{C_s}{C_e} \tag{10}$$

where, a_s is the activity of adsorbed ER, a_e the activity of the ER in solution at equilibrium, C_s the amount of ER adsorbed by per unit mass of catalyst (mmol/g), C_e the ER concentration in solution at equilibrium (mmol/ml), f_s the activity coefficient of the adsorbed ER and f_e is the activity coefficient of the ER in solution at equilibrium. As the ER concentration in the solution decreases and approaches zero, K_0 becomes equivalent to ln C_s/C_e at C_0 [17]. Therefore, K_0 can be approximated by extrapolating C_s to zero in ln C_s/C_e versus C_s curve (Fig. 4). The K_0 value so obtained, is related to the standard adsorption
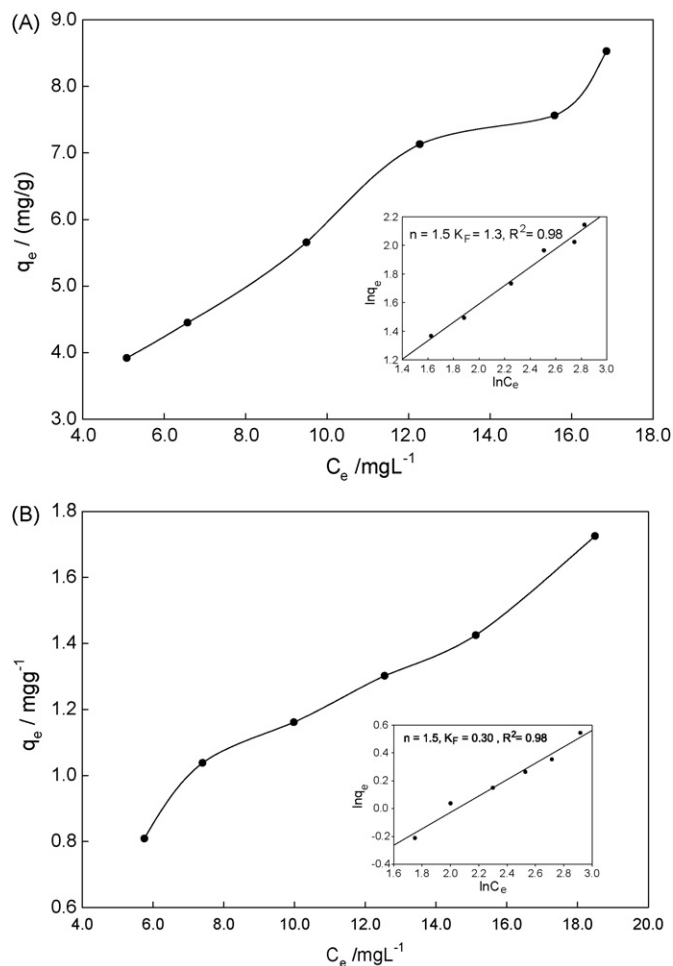

Fig. 3. Study of Freundlich adsorption isotherm. (A) Adsorbent; TiO$_2$ (pH, 6.0) and (B) adsorbent; ZnO (pH, 6.0) at room temperature.

free energy ($\Delta_{ad}G°$) by the well-established thermodynamic Eq. (11):

$$\Delta_{ad}G° = -RT \ln K_0 \tag{11}$$

where, R is the universal gas constant (8.314 J K^{-1} mol^{-1}) and T is the temperature in Kelvin scale. The negative value of $\Delta_{ad}G°$ and positive value (confirmed by the decrease of temperature) of standard adsorption enthalpy ($\Delta_{ad}H°$) indicates that the adsorption (Table 2) of ER on TiO$_2$ or ZnO surface is a endothermic spontaneous process with increasing standard adsorption entropy ($\Delta_{ad}S°$) defined by the Eq. (12):

$$\Delta_{ad}G° = \Delta_{ad}H° - T\Delta_{ad}S° \tag{12}$$

Table 1
Adsorption and decolorization related constants for TiO$_2$ and ZnO mediated processes (R^2 value in the parenthesis)

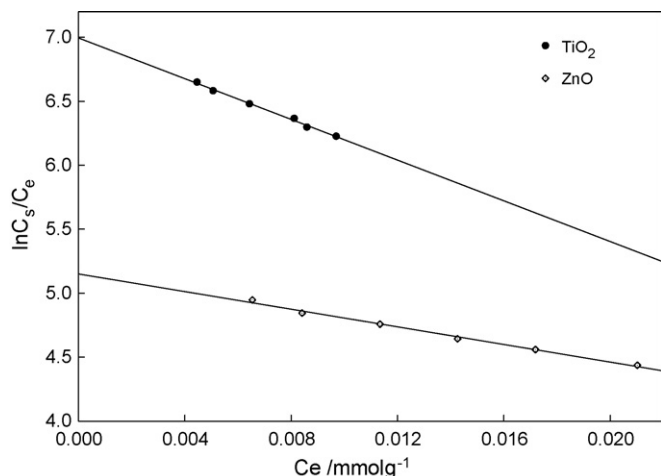| Catalyst	Freundlich constants		Langmuir constants		L–H constants	
	K_F	n	K' (mg/g)	k_1 (L/mg)	K (L mol^{-1})	k (mol L^{-1} min^{-1})
TiO$_2$	1.30	1.5 (R^2; 0.98)	17.54	0.54 (0.97)	2.78×10^7	1.79×10^{-8} (0.94)
ZnO	0.30	1.5 (R^2; 0.98)	3.06	0.17 (0.96)	1.66×10^7	1.67×10^{-8} (0.93)

Fig. 4. Approximation of equilibrium adsorption constant K_0 for ER–TiO$_2$/ZnO dispersions. Temperature: 298 K and medium pH 6.0.

Table 2
Relative thermodynamic parameters for TiO$_2$ and ZnO mediated processes (R^2 value in the parenthesis)

Catalyst	Equilibrium adsorption constant, K_0	$\Delta_{ad}G^\circ$ (kJ mol^{-1})	$\Delta_{ad}H^\circ$	$\Delta_{ad}S^\circ$
TiO$_2$	6.99 (0.99)	−4.83	Positive	Positive
ZnO	5.15 (0.99)	−4.01	Positive	Positive

Even tough we have not done temperature dependant experiments, the thermodynamic approximation delineates that the adsorption efficiency on TiO$_2$ could be accelerated by the increased temperature. The $K_{F(TiO_2)} > K_{F(ZnO)}$ and $\Delta_{ad}G^\circ$ (TiO$_2$) > $\Delta_{ad}G^\circ$ (ZnO) indicates that TiO$_2$ shows better adsorption performance over ZnO.

3.2. Optimization of catalyst loading on decolorization rate

Decolorization/degradation rate of organic molecules takes place on active surface of the catalyst particles followed by adsorption.

Bekbolet et al. [18] found that 4 g/L of TiO$_2$ was the most effective catalyst dosage for decolorization and noticed that over this concentration the suspended particles of TiO$_2$ block the UV-light passage and reduce the formation of electron–hole pairs and active sites. Garcia et al. [19] found that 8 g/L of TiO$_2$ loading was most efficient in decolorization and mineralization of imazaquin in UV radiation. Alhakimi et al. [20] reported that a catalyst loading of 3 g/L was found to be optimum for potassium hydrogen phthalate decolorization using TiO$_2$ and solar light. The results cited above clarify that a maximized catalyst dosage is not a general phenomenon for all photocatalytic decolorization and it is definitely subject to various experimental parameters, for example, type of the adsorbent and adsorbate medium temperature, pH etc maintained for a specific process. The photocatalytic activities of semiconductors are also dependent on the crystalline, particle size, surface area of the adsorbents and concentration of the impurities in the catalysts [18–21].
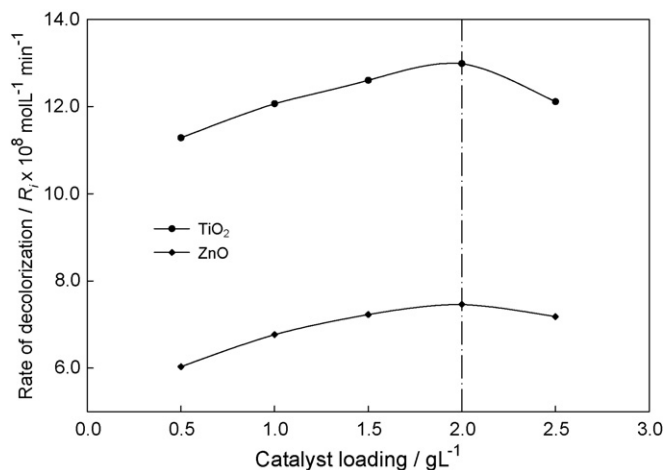

Fig. 5. Effect of catalyst loading on decolorization rate for fixed ER concentration in presence of UV radiation. Initial ER concentration: 22.0 μM and medium pH 6.0. Temperature: 298 K.

In order to optimize the catalyst loading in our experimental condition, series of experiments were carried out by impregnating variable catalyst loading (0.5–2.5 g/L) in presence of 22.0 μM ER solution at 299 K. The influence of the catalyst loading has been explained by calculating initial rate of decolorization (R_i) using Eq. (13):

$$R_i = \frac{-d[ER]}{dt} \tag{13}$$

The results sketched in Fig. 5 indicate that TiO$_2$ has greater decolorization efficiency over ZnO. In each of the case, R_i increases upto a maxima as a function of catalyst loading and tends to decrease upon further loading. The increasing trend of R_i with catalyst loading is related to the facts that (a) catalyst loading increases the total surface area of the catalyst for ER to be adsorbed (b) the increased amount of catalyst produces proportional amount of $^\bullet$OH radicals by absorbing increased numbers of photons which are sufficient and readily accessible to nearby ER to decolorize [18–21]. The optimum catalyst loading was found 2.0 g/L in our case for both catalysts. However loadings, higher than 2.0 g/L, could not further accelerate the decolorization efficiency because (i) agglomeration might have taken place which must reduce the total active surface area to adsorb ER and to absorb UV radiation in order to promote R_i of ER (ii) higher concentration of catalyst created turbidity. Turbidity is capable to reduce the penetration intensity of UV radiation by the scattering effect [18–20].

3.3. Influence of pH on decolorization rate

The solution pH exhibits an interesting influence on the oxidation potential and surface charge of the semiconductor type catalysts. The surface charge of TiO$_2$ or ZnO has a significant effect on the adsorption and decolorization of the dye molecules [7,10,22]. In our research, the effect of pH on the decolorization rate was studied in the pH range of 5.5–10.0 using 7.0 μM of ER and 0.5 g/L of each catalyst. The solution pH was adjusted just before the irradiation to be started and no buffered system was
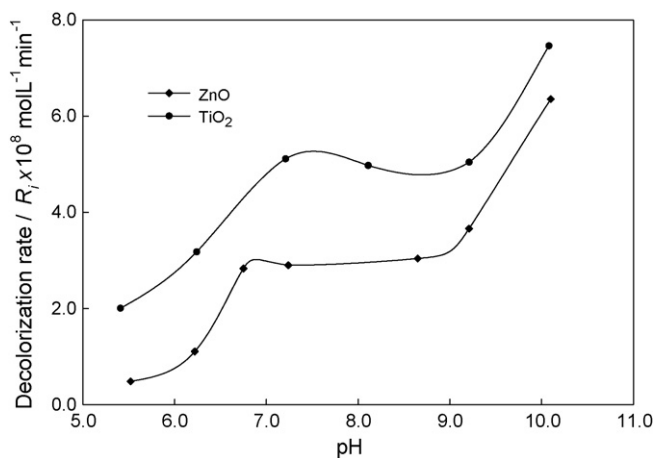
Fig. 6. Influence of pH on decolorization rate of erythrosine over TiO$_2$/ZnO surface in presence of UV radiation. Initial ER concentration: 7.0 μM; catalyst loading: 0.50 g/L; medium temperature: 298 K.

Table 3
Effect of H$_2$O$_2$ on decolorization rate ($r \times 10^8$ mol L^{-1} min^{-1}), ER; 7.0 μM

ER (no catalyst)	1.37
4.0×10^{-2} M, H$_2$O$_2$	2.83
TiO$_2$ (0.5 g/L)	2.31
TiO$_2$ (0.5 g/L) and 4.0×10^{-2} M, H$_2$O$_2$	5.80
ZnO (0.5 g/L)	2.10
ZnO (0.5 g/L) and 4.0×10^{-2} M, H$_2$O$_2$	4.80

used to maintain a constant pH during the course of reaction. Fig. 6 shows that the R_i was increased as the medium pH was increased from 5.0 to 7.0 and remained steady up to 9.0. The further increase of pH from 9.0, R_i tended to increase again. This interesting behavior can be explained by the acid–base properties of the metal oxide surfaces whose photocatalytic activities are determined by their zero point charge (ZPC). ZPC of TiO$_2$ and ZnO are at pH of 6.5 and 10.0 [21,22], respectively. Semiconductor type catalyst surface is negatively and positively charged above and bellow this pH accordingly. Therefore, it can be estimated that pH, lower than ca. 6.0 both TiO$_2$ and ZnO surfaces were too covered by ER molecules to be effectively penetrated by the UV radiation. This improper penetration reduced the $^{\bullet}$OH radical generation to decrease the R_i. In the pH range ca. 7.0–9.0, both catalysts might have fixed catalytic sites porn to UV radiation to cause decolorization showing a steady R_i. At very higher pH, the accelerated rate of decolorization is conflicting since ER is an anionic dye. Primarily, we thought that higher rate of decolorization was probably due to some structural changes of ER molecules similar as the action of acid-base indicator. Therefore, we investigated the stability of pH dependant ER spectrum. We found that UV–vis absorption spectrum of ER is quite stable in the pH range of 5.0–11.0. So, it was obvious that decolorization was occurred due to some chemical changes.

At higher pH (above ZPC), quantitatively, excessive amount of adsorbed hydroxyl (–OH) ions are present on catalytic surface [10]. Therefore, the further increase of pH from ca. 9.0, favors the formation of excessive $^{\bullet}$OH radicals in presence of UV radiation which are considered as the major oxidant to accelerate the R_i of dye molecules [23,24].

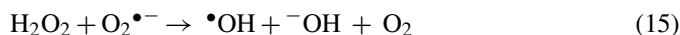### 3.4. Influence of H$_2$O$_2$ on decolorization of rate

The R_i of organic compounds can significantly be improved either in the presence of oxygen or by the addition of hydrogen peroxide [25]. To verify the influence of H$_2$O$_2$ over initial rate of decolorization, we have conducted several experiments taking 7.0 μM ER solution. We irradiated (a) aqueous ER only, (b)

ER with 4.0×10^{-2} M H$_2$O$_2$, (c) ER with catalyst (0.5 g/L) and (d) ER with the mixture of catalyst (0.5 g/L) and 4.0×10^{-2} M H$_2$O$_2$. The result thus obtained is reported in the Table 3. The R_i was found to be very slow for dye alone but in presence of H$_2$O$_2$, the decolorization phenomena is slightly better and in presence of both TiO$_2$/ZnO and H$_2$O$_2$, the rate of decolorization was accelerated at a remarkable extent. This effect of H$_2$O$_2$ can be explained by radical reaction mechanism [25] (Eqs. (14)–(16)). The added H$_2$O$_2$ can scavenge electrons from conduction band of TiO$_2$/ZnO to generate excess hydroxyl radicals. The H$_2$O$_2$ molecules can also generate hydroxyl radicals by direct homolytic fission in presence of UV-light:

$$H_2O_2 + (TiO_2/ZnO)e^- \rightarrow {}^{\bullet}OH + {}^-OH \quad (14)$$

$$H_2O_2 + O_2^{\bullet -} \rightarrow {}^{\bullet}OH + {}^-OH + O_2 \quad (15)$$

$$H_2O_2 + h\nu \rightarrow 2{}^{\bullet}OH \quad (16)$$

As mentioned earlier, $^{\bullet}$OH radicals are the major oxidant for dye decolorization, therefore, the excess $^{\bullet}$OH radicals so added to the system, accelerated the decolorization rate.

3.5. Decolorization kinetics

Investigation of kinetics of dye decolorization is often confusing because the process is complex. It is often believed that degradation mechanism follows first-order kinetics [7,10,11]. In order to investigate kinetics of the present study, initial ER concentration dependant experiments were performed. We compared our data for first order and zero-order kinetics, respectively.

If there is a single active-site involved on the catalyst surface, the surface coverage (θ) is expressed by Eq. (17) where K is the adsorption constant:

$$\theta = \frac{K[ER]}{1 + K[ER]} \quad (17)$$

The related surface catalytic reaction rate can be expressed by Eq. (18) according to Langmuir–Hinselwood (L–H) mechanism where, k is the rate constant:

$$-\frac{d[ER]}{dt} = r = k \frac{K[ER]}{1 + K[ER]} \quad (18)$$

The reciprocal of Eq. (18) provides a linear relationship between rate of reaction and equilibrium concentration of ER (Eq. (19)):

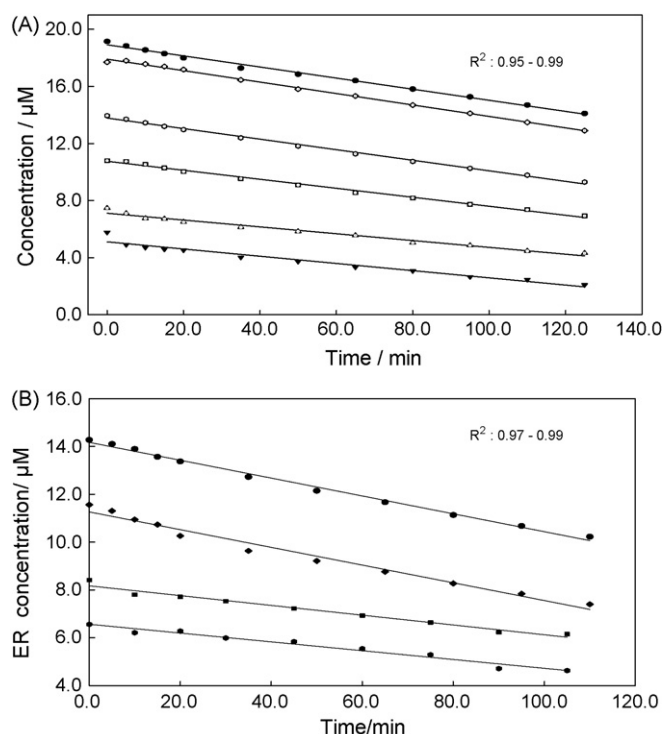$$\frac{1}{r} = \frac{1}{kK[ER]} + \frac{1}{k} \quad (19)$$

Fig. 7. Linearity test of decolorization kinetics of ER over TiO$_2$ and ZnO surfaces in presence of UV radiation at various ER concentrations. Catalyst loading: 0.50 g/L and medium temperature: 298 K. Medium pH: 6.0. (A) TiO$_2$ and (B) ZnO.

The constants k and K, calculated from the slope and intercept of the Eq. (19) has been listed in the Table 1. If the ER concentration is very low ($\theta \ll 1$), it means that $1 \gg K[\text{ER}]$ in the denominator of Eq. (18) because K has the large value of 2.78×10^7 and 1.66×10^7 L mol^{-1} for TiO$_2$ and ZnO, respectively. Therefore, the Eq. (18) is rendered into the differential form of the first-order rate Eq. (20):

$$r \cong kK[\text{ER}] = k_a[\text{ER}]^1 \tag{20}$$

where, k_a is the apparent first order rate constant and the integrated form of first order rate is given by Eq. (21):

$$[\text{ER}]_t = [\text{ER}]_0 \, e^{-k_a t} \tag{21}$$

Similarly, relatively higher ER concentration ($\theta \cong 1$) implies that $1 \ll K[\text{ER}]$ leading to the conversion of Eq. (18) into a zero order rate equation whose differential and integrated forms are given by Eqs. (22) and (23), respectively

$$r \cong k_a[\text{ER}]^0 \tag{22}$$

$$[\text{ER}]_t = [\text{ER}]_0 - k_a t \tag{23}$$

A plot of $[\text{ER}]_t$ vs irradiation time (t) thus should give an exponential curve if the reaction mechanism follows first-order kinetics (Eq. (21)) and if the mechanism is zero-order kinetics the plot should be a straight line (Eq. (23)). In our case we found straight lines (R^2; 0.95–0.99) when we plotted $[\text{ER}]_t$ against irradiation time (t) as shown in Fig. 7. This means that the decolorization mechanism of ER under our reaction condition followed zero-order kinetics over TiO$_2$/ZnO surface. We

used the ER concentration range of 7.0–22.0 μM over constant catalyst loading i.e. 0.5 g/L TiO$_2$/ZnO for this study. Probably this concentration range is sufficient to form a mono layer coverage ($\theta \cong 1$) over TiO$_2$ or ZnO surface (formation of multilayer were also inferred from Freundlich isotherm study). So it can be inferred that further lower concentration of ER apart from this range may follow first order kinetics. The observation of zero-order kinetics was further confirmed by calculating half life ($t_{1/2}$) and the rate constants k_a of the decolorization process.

If the decolorization mechanism follows first-order kinetics, Eq. (21) implies that the $t_{1/2}$ should be constant disregarding the initial ER concentration (Eq. (24)):

$$t_{1/2} = \frac{\ln 2}{k_a} \tag{24}$$

On the other hand, according to (23), the zero order $t_{1/2}$ is proportional to the initial dye concentration (Eq. (25)):

$$t_{1/2} = \frac{1}{2} \frac{[\text{ER}]_0}{k_a} \tag{25}$$

Based on Eqs. (24) and (25), the concentration dependant half lives ($t_{1/2}$) reported in Fig. 8 shows that calculated
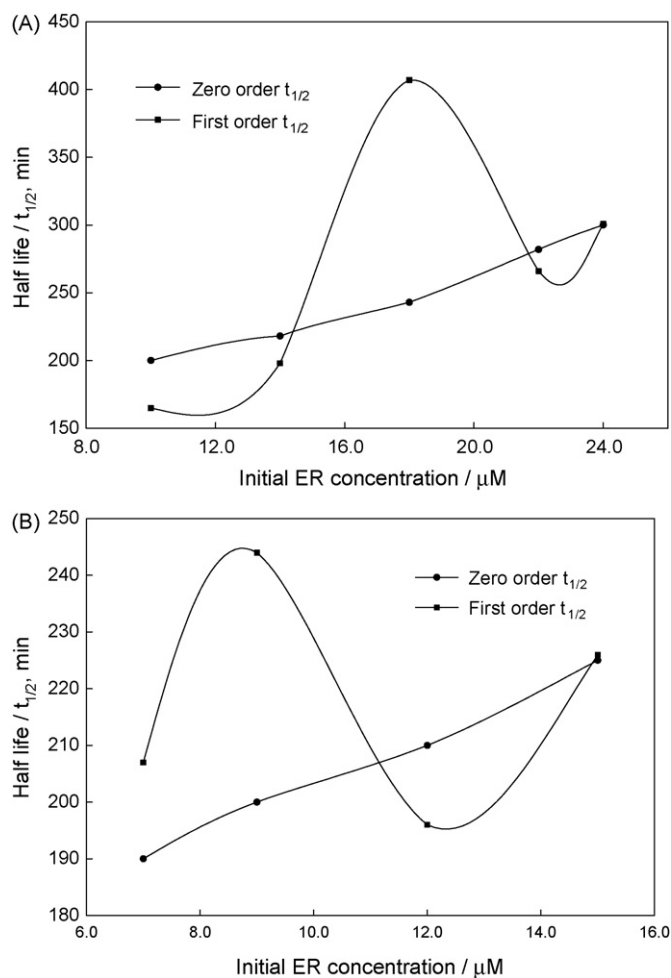

Fig. 8. Zero order and first order decolorization half lives ($t_{1/2}$) of ER over catalyst surface: (A) TiO$_2$ and (B) ZnO. Catalyst loading: 0.50 g/L and medium temperature: 298 K. Medium pH: 6.0. (A) TiO$_2$ and (B) ZnO.

$t_{1/2}$ (zero order) is absolutely proportional to the initial ER concentration but calculated $t_{1/2}$ (first order kinetics) is irregularly dependant on initial ER concentration for both catalysts. Therefore, it can be concluded that under our experimental condition, ER decolorization process manifested zero-order kinetics.

4. Conclusion

The adsorption and degradation of erythrosine was carried out over TiO_2 and ZnO surfaces. The data obtained is well fitted with Freundlich and L–H adsorption isotherms. The approximated thermodynamic parameters revealed the fact that the adsorption process is an endothermic spontaneous process. Catalytic loading has an optimum condition to enhance decolorization rate and 2.0 g/L was found as the most effective dosage. Increasing pH favors the decolorization rate because of favorable surface properties. H_2O_2 influences positively the decolorization rate as it can provide excess OH radicals. Under all experimental conditions TiO_2 showed better catalytic properties over ZnO subject to both adsorption and decolorization. Under the experimental condition described, it was noticed that decolorization mechanism of ER follows a zero-order kinetics over TiO_2/ZnO surfaces.

Acknowledgements

References

[1] E.V. Hess, Toxicology 181–182 (2002) 65–70.
[2] I. Poulios, D. Makri, X. Prohaska, Global Nest Int J. 1 (1999) 55–62.
[3] U. Pagga, D. Brown, Chemosphere 15 (1986) 1479–1491.
[4] M. Katoh, H. Aihara, T. Horikawa, T. Tomida, J. Colloid Interface Sci. 298 (2006) 805–809.
[5] C. Minero, D. Vione, Appl. Catal. B: Environ. 67 (2006) 257–269.
[6] G. Wang, F. Wu, X. Zhang, M. Luoc, N. Deng, J. Hazard. Mater. 133 (2006) 85–91.
[7] M.A. Behnajady, N. Modirshahla, R. Hamzavi, J. Hazard. Mater. 133 (2006) 226–232.
[8] W.-Y. Wang, Y. Ku, Water Res. 40 (2006) 2249–2258.
[9] S. Anandana, A. Vinub, N. Venkatachalam, B. Arabindoo, V. Murugesan, J. Mol. Catal. A: Chem. 256 (2006) 312–320.
[10] M.A. Hasnat, I.A. Siddiquey, A. Nuruddin, Dyes Pigments 66 (2005) 185–188.
[11] M.A. Hasnat, I.A. Siddiquey, S.M. Saiful Islam, Indian J. Chem. 42A (2002) 1865–1867.
[12] W. Taixing, L. Guangming, Z. Jincai, H. Hisao, S. Nick, J. Phys. Chem. B 103 (1999) 4862–4867.
[13] A. Mittal, J. Mittal, L. Kurup, A.K. Singh, J. Hazard. Mater. B 138 (2006) 95–105.
[14] Y. Yang, Y. Guo, C. Hu, C. Jiang, E. Wang, J. Mater. Chem. 13 (2003) 1686–1694.
[15] T. Wu, T. Lin, J. Zhao, H. Hidaka, N. Serpone, Environ. Sci. Technol. 33 (1999) 1379.
[16] M. Pera-Titus, V.G. Molina, M.A. Banos, J. Gimenez, S. Esplugas, Appl. Catal. B 47 (2004) 219–256.
[17] R. Niwas, U. Gupta, A.A. Khan, K.G. Varshney, Colloid Sur. Physicochem. Eng. Asp. 164 (2000) 115–119.
[18] M. Bekbolet, G. Ozkosemen, Water Sci. Technol. 3 (1996) 189–194.
[19] J.C. Garcia, K. Takashima, J. Photochem. Photobiol. A: Chem. 155 (2003) 215–222.
[20] G. Alhakimi, L. Studnicki, M. Al-ghazali, J. Photochem. Photobiol. A: Chem. 154 (2003) 219–228.
[21] M. Muruganandham, M. Swaminathan, J. Hazard. Mater. B135 (2006) 78–86.
[22] S. Sakthivel, B. Neppolian, M. Palanichamy, B. Arabindoo, V. Murugesan, Indian J. Chem. Technol. 6 (1999) 161.
[23] M. Muruganandham, M. Swaminathan, Sol. Energy Mater. Sol. Cells 81 (2004) 439.
[24] A.A. Khodja, T. Sehili, J.F. Pilichowski, P. Boule, J. Photochem. Photobiol. A: Chem. 141 (2001) 231.
[25] I. Poulios, D. Makri, X. Prohaska, Global Nest Int. J. 1 (1) (1999) 119–130.